Eur. Phys. J. D **9**, 123–126 (1999)

THE EUROPEAN PHYSICAL JOURNAL D
EDP Sciences

Near-threshold photoionization of germanium clusters in the 248–144 nm region: ionization potentials for Ge_n

K. Fuke[a] and S. Yoshida

Department of Chemistry, Kobe University, Nada-ku, Kobe 657-8501, Japan

Received: 2 September 1998

Abstract. We examine the photoionization thresholds of Ge_n $(n = 2 - 34)$ with a wide photon energy (5.0–8.6 eV) using a laser photoionization time-of-flight mass spectrometry. A high-output vacuum ultraviolet light generated with stimulated Raman scattering is used as the ionization light source in the energy above 6.0 eV. A characteristic size dependence of ionization potential (IP) with a maximum at $n = 10$ is found for clusters smaller than 22 atoms. The rather high IP of Ge_{10} in comparison with its neighbors is consistent with the results on the photodissociation study of Ge_n^+. We also find that IPs decrease rapidly from $n = 16$ to 22, and then decrease at a much slower rate for larger clusters. These features in IPs are similar to those of Si_n reported in our previous paper, except for the smaller IP gap of Ge_n at $n \approx 20$. We discuss these results on IPs in relation to their electronic structure and stability.

PACS. 36.40.Mr Spectroscopy and geometrical structure of clusters – 71.24.+q Electronic structure of clusters and nanoparticles

1 Introduction

The structures and properties of small semiconductor clusters have been the subject of intensive study because of their importance in both fundamental and applied sciences. These studies include the reactivities of Si_n toward small molecules such as O_2, NH_3, C_2H_4, etc. [1–3]. Photodissociation [4–6] and collision-induced dissociation [7] experiments have also been conducted, so that information on the stabilities and binding energies of Si_n and Ge_n may be gained. However, little is known about the structures of silicon clusters. Recently, Jarrold and others have measured the mobilities of Si_n^+ and Ge_n^+, using injected-ion drift-tube techniques to obtain information on the structures of these clusters [8, 9]. The results of Si_n^+ indicate the existence of isomers having different mobilities and the occurrence of a structural transition between these isomers. Although they have made substantial progress in obtaining the gross structures of cluster ions, it has not yet been possible to obtain detailed experimental information on the structures of Si_n and Ge_n, and thus, most of what we know about the structures comes from theoretical calculations [10–14].

In order to gain information on the growth of the electronic-level structure of semiconductor clusters, photoelectron spectroscopy [15–19] of negatively charged silicon and germanium clusters, and electronic absorption spectroscopy [20, 21] of size-selected clusters have been conducted. Other physical properties, such as ionization potentials (IPs) are also important for understanding the electronic structure, chemical reactivities, and dissociation processes. In our previous papers [22, 23], we have reported the photoionization thresholds of Si_n, $n = 2 - 200$. The IPs have been found to exhibit a large gap in between $n = 20$ and 22. This gap has been tentatively ascribed to the structural transition of neutral silicon clusters in analogy with that of the cluster ions observed recently in the mobility measurements [8].

In the present work, we examine the photoionization thresholds of Ge_n, $n = 2 - 34$ in the energy region of 5.0–8.6 eV to obtain further information on the size dependence of IPs for semiconductor clusters. In the energy region above 6.42 eV (ArF laser), high-output vacuum ultraviolet (VUV) laser light, generated by anti-Stokes (AS) conversion, is used as the photoionization light source to bracket the IPs.

2 Experimental methods

Clusters of germanium atoms are produced using a laser vaporization source [23]. A pulsed, frequency-doubled Nd:YAG laser (ca. 10 mJ/pulse) is focused onto the surface of a 0.6-cm-diameter germanium rod, which is translated and rotated within an aluminum source block. Germanium atoms evaporated from the rod surface are mixed with helium and flowed into a cylindrical flow tube (5 cm long by 0.35 cm i.d.), where cooling and cluster growth occur. To produce cold clusters, the tube is maintained

[a] e-mail: fuke@kobe-u.ac.jp

at about 80 K by a liquid nitrogen-cooled copper block surrounding the tube. Germanium clusters thus produced are collimated with a skimmer and are introduced to the ion extraction region of a time-of-flight (TOF) mass spectrometer, where the clusters are photoionized. For the photoionization measurement, we use the reflectron TOF mass spectrometer described in our previous paper [23].

Clusters are photoionized with a VUV laser light in the 5.9–8.5 eV energy region. The VUV light is generated by anti-Stokes (AS) conversion of narrow-bandwidth UV radiation at 193, 248, and 266 nm. For example, in the photoionization experiments with 248 nm radiation, the frequency-doubled output (typically 0.2 mJ/pulse) of an Nd:YAG pumped-dye laser (Quanta-Ray, GCR-250, and PDL-3; Coumarine 500) is amplified by a KrF excimer laser (Lambda Physik COMPex 100) after collimating by two plano-convex lenses. The energy from the entire system is typically 10 mJ/pulse at 248 nm. The amplified output is focused into an H_2 Raman cell. The radiation leaving the cell through an MgF_2 window is dispersed by a rotatable 30° CaF_2 prism, and is introduced to the ionization region of the mass spectrometer through an evacuated tube, in which several slits are placed to feed a given order of the AS components. Various AS and Stokes components thus generated are used as the photoionization light source in the energy region above 5.9 eV. Although we did not measure the absolute energy of the VUV light, it is estimated to be less 10 μJ/pulse at 144 nm (H_2, 7th AS component of 248 nm radiation) from the comparison of the signal intensities of Ge_{22-25} cluster ions produced by irradiation of attenuated 193 nm light. The ionization laser fluence was attenuated as low as possible to avoid multiphoton ionization and dissociation processes.

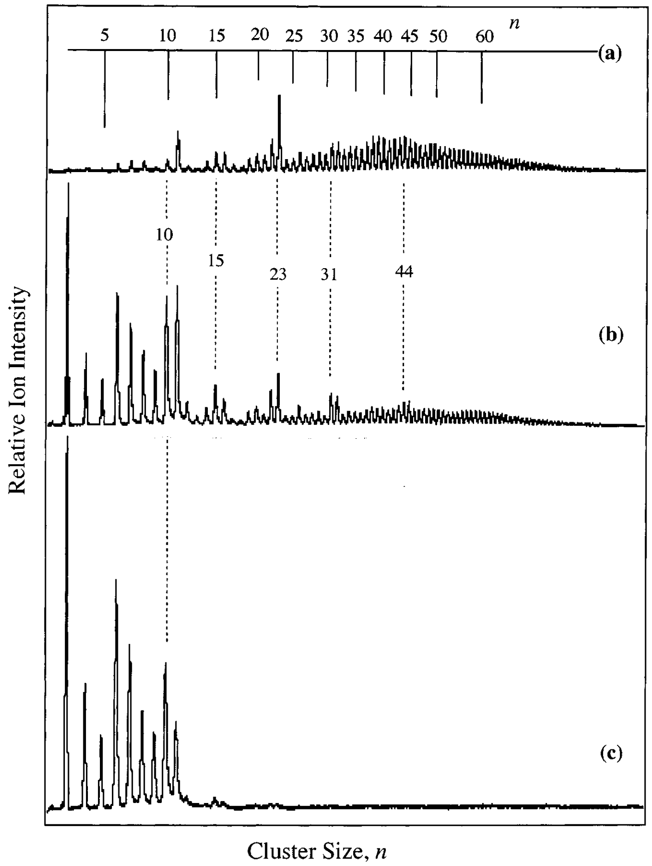

Fig. 1. Photoionization mass spectra of germanium clusters, Ge_n, $n = 1-100$, recorded with various laser fluences at 6.42 eV (ArF): (a) 20 μJ/cm^2; (b) 0.5 mJ/cm^2; and (c) 2 mJ/cm^2.

3 Results and discussion

Silicon and germanium clusters have known to exhibit efficient photofragmentation processes [4–6, 23], which disturb an accurate determination of the ionization thresholds of small clusters. In order to confirm the size, where the cluster is one-photon ionized at 6.42 eV (193 nm), we measured the photoionization mass spectrum with various laser fluences ranging from 2–500 μJ/cm^2. From the analysis of these spectra, germanium clusters with equal to and more than 19 atoms are found to be photoionized by the one-photon process at 6.42 eV. Figure 1 shows the typical photoionization mass spectra of Ge_n produced with various laser fluences. In addition to the clusters with $n \geq 19$, we also observe the fragment ions such as Ge_6^+, Ge_7^+, Ge_{11}^+, Ge_{14}^+, Ge_{15}^+, and Ge_{16}^+; even the laser fluence is attenuated to 20 μJ/cm^2, as shown in Fig. 1a. When the clusters are photoionized without cooling of the cluster source, this trend becomes quite prominent. With increasing laser fluence, the ion signals of larger clusters ($n > 20$) decrease gradually, while those of Ge_n^+ ($n = 6-11$, 14, 15, 23, 31, 32) become increasingly prominent and exhibit magic behavior. These cluster ions are produced through a fission-type fragmentation after multiphoton absorption [4–6], and some of them have also been observed as magic ions in quenched Ge vapor [24]. At the laser fluence of 2 mJ/cm^2, only the clusters with $n \leq 11$ are detected, as shown in Fig. 1c. The extensive fragmentation of Ge_n^+ has also been observed at 157 nm by Smalley's group [25]. In our previous papers [22, 23], we have studied the photoionization process of Si_n clusters at various wavelengths, including the VUV radiation. Although Si_n^+ also exhibit the extensive fragmentation process, no such clear magic behavior has been observed with the medium laser fluence. The reason why Ge_n^+ exhibit clear magic behavior may be due to their weaker binding energies as compared with those of Si_n^+ [9].

Figure 2 shows the TOF mass spectra of Ge_n ($n = 2-30$) clusters produced at 7.46, 7.58, and 7.76 eV, which correspond to the AS-2, AS-5, and AS-6 lines of the 193, 248, and 266 nm radiation, respectively. In the energy region above 7.58 eV, the ion signals of Ge_6^+, Ge_7^+, and Ge_{10}^+ become prominent. The aforementioned fact that Ge_6^+, Ge_7^+, and Ge_{10}^+ readily contaminate the mass spectrum hampers the determination of the IPs of these clusters. As shown in Figs. 2a and 2b, very weak signals of these clusters are observed, in addition to those of $n \geq 8$. However, the ion signals of these clusters increase rapidly from 7.58 to 7.76 eV, as seen in Fig. 2c. These results, as well as the careful examination of the intensity of these ions relative

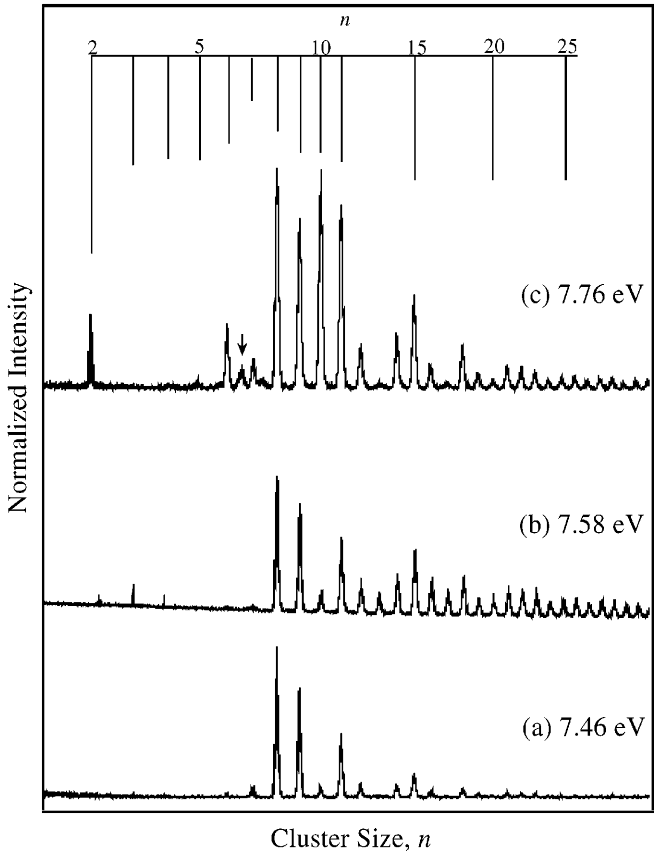

Fig. 2. A series of germanium cluster photoionization mass spectra taken at the indicated energies; (a), (b), and (c) correspond to the AS-2, AS-5, and AS-6 lines of the 193, 248, and 266 nm radiation, respectively. The ion signal marked by an arrow cannot be assigned.

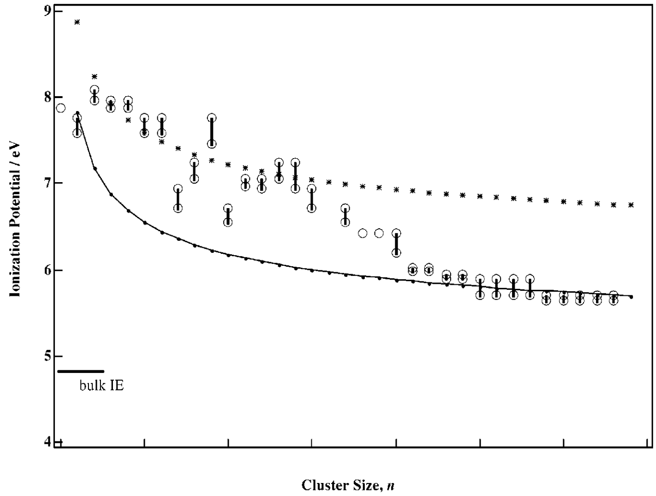

Fig. 3. Ionization potentials of Ge_n, $n = 2-34$, plotted versus n with open circles. Bulk ionization energy (IE) for Ge is indicated by a solid line. The solid line connecting the closed circles represents the prediction of the spherical droplet model with the reported bulk IE (4.80 eV), while * indicates the predicted values, which is intentionally shifted by 1 eV.

to that for Ge_{22-30} in the mass spectra produced at several ionization energies, allow 7.58–7.76 eV to be placed on the IP of Ge_6, Ge_7, and Ge_{10}. We also see the weak ion signals of Ge_4^+ and Ge_5^+ in Fig. 2c, but these signals are not detected in the mass spectrum produced with the F_2 laser at 157 nm (7.87 eV, about2 $\mu J/cm^2$). The latter result clearly indicates that Ge_{3-5} have IPs higher than this energy. From the similar analysis of mass spectra produced at energy higher than 7.76 eV, we determine the IPs of Ge_4^+ and Ge_5^+ as $7.87-7.97$ and 7.87–7.97 eV, and those of Ge_2 and Ge_3 as $7.58-7.76$ and 7.97–8.09 eV, respectively.

It is worth noticing that the peak intensity of Ge_{10}^+ is rather high, compared with its neighbors, as can be seen in the mass spectrum shown in Fig. 2c. Although it is not shown, this trend is found to become very evident in the mass spectrum produced at higher photon energy. Since these spectra are recorded at low laser fluence to suppress multiphoton processes (about 4 $\mu J/cm^2$) and with energy higher than the ionization thresholds of Ge_n ($n = 6$), the abundance of neutral clusters may be reflected in the intensities of each cluster ion. The spectrum thus indicates that Ge_{10} is more stable than its neighbors. As for Ge_{10}, the photodissociation [5] and collision-induced dissociation [9] experiments of Ge_n^+ suggest that this cluster is a favored neutral product. These results are consistent with the present observation for Ge_{10}. In the previous work on Si_n [23], we have found similar magic behavior at Si_{10}. As for the latter clusters, Raghavachari and Rohlfing [8] have reported detailed calculations on the binding energies of Si_n with $n = 2-10$, and have predicted the special stability of this cluster.

We also carry out similar photoionization experiments with the second harmonic of the excimer pumped-dye laser in the wavelength region of 206–224 nm. It is rather difficult to determine the threshold ionization energy accurately for larger clusters with $n > 21$, because of the lowering of the photoionization cross section and the clusters' relative abundances in the beam. Thus, in the present work, the IPs of the clusters with $21 \le n \le 34$ are roughly bracketed.

The IPs for Ge_{2-34} determined in the present work are plotted against n in Fig. 3. As mentioned previously, the IPs for Ge_2 and Ge_3 are found to be $7.58-7.76$ and 7.97–8.09 eV, respectively, and the IP of Ge_3 is close to that of the Ge atom (7.88 eV). Up to now, three theoretical groups have examined the ionization potentials of small germanium clusters. Dixon and Gole [26] have calculated the electronic structure of Ge_3 with a local density functional approximation and determined the adiabatic IP as 8.28 eV. They have also predicted a large geometrical change between the $^1A_1$ neutral ground state and the $^2B_2$ cation. Thus, the calculations seem to slightly overestimate the IP of Ge_3. For Ge_4 and Ge_5, Dai and Balasubramanian [27] have estimated the adiabatic IPs as 7.44 and 7.50 at the multireference singles + doubles configuration interaction level of theory, while the vertical IPs of these clusters determined here are 7.87–7.97 eV. According to their calculations, both Ge_4 and Ge_4^+ have the equilibrium structure of a rhombus, but their acute apex angles are quite different. Taking into account the geometrical change, the theoretical values may agree reasonably well with the present results. Quite recently, Jo and Lee [28] have also reported the IPs of Ge_n ($n = 2-12$) calculated with the parameterized Hamiltonian method. However, their IPs are more than 2 eV higher than those determined in this work.

As shown in Fig. 3, the IPs of Ge_n decrease gradually with a major peak at $n = 10$. The rather high IP of Ge_{10} is consistent with the results on the photodissociation study [7] of Ge_n^+. Although the abundance of the product cluster ions is also affected by the dynamics of dissociation, the fragment cluster, having a lower IP, has a tendency to be charged in the fission-type dissociation of energized cluster ions; for example, Ge_9^+ and Ge_{11}^+ are produced predominantly in the dissociation process of Ge_{19}^+ and Ge_{21}^+, respectively [5]. If we take into account this tendency, the photodissociation results [5] may suggest that Ge_{10} has the lowest IP among three clusters, e.g., Ge_6, Ge_7 and Ge_{10}, whose IPs are bracketed in 7.58–7.76 eV, as mentioned previously. In Fig. 3, the results, based on a classic conducting spherical droplet (CSD) model, are also depicted with a solid line; the cluster IP is assumed to converge to the bulk work function (4.80 eV [29]), and the cluster radius R is estimated from the bulk density. This model often reproduces well the experimentally measured IPs for metal clusters such as Na_n and K_n. As seen in Fig. 3, the IPs of Ge_n with $n < 18$ deviate significantly from this model, while Ge_n with $n \geq 22$ seem to follow the line. The preliminary results on Ge_{35-60} show that the IPs decrease gradually to about 5.6 eV. On the other hand, the IPs of Ge_{18-21} decrease at a much faster rate. This feature in the size dependence of IPs for Ge_n is rather similar to that found for Si_n: a large gap in IP (about 1.5 eV) between Si_{20} and Si_{22} has been observed [23]. In the case of Si_n, we have tentatively ascribed the IP gap to the occurrence of the structural transition similar to that found for Si_{24}^+–Si_{34}^+, which has been detected in the mobility measurements by Jarrold and Constant [8]. Jarrold and his group have also examined the structures of Ge_n^+ using the same technique; however, they have found no structural transition for Ge_n^+ with $n = 7-54$, except for Ge_{40}^+ [9]. One of the possible reasons why no clear structural transition is detected for Ge_n^+ in this size range may be the much lower potential barrier for isomerization. At the moment, we have no definitive interpretation for the IP gap of Ge_n. To get further insight into this issue, elaborate theoretical calculations for both the geometries and electronic structures of Si_n and Ge_n clusters with 20 to 30 atoms are necessary.

This work was partially supported by Grants-in-Aid from the Ministry of Education, Science, Sports, and Culture of Japan. We are also grateful to the Aichi Science and Technology Foundation and the Japan Society for the Promotion of Science for financial support.

References

1. M.F. Jarrold: Science **252**, 1085 (1991), and references cited therein
2. J.M. Alford, R.T. Laaksonen, R.E. Smalley: J. Chem. Phys. **94**, 2618 (1991); J.L. Elkind, J.M. Alford, F.D. Weiss, R.T. Laaksonen, R.E. Smalley: J. Chem. Phys. **87**, 2397 (1987)
3. M.L. Mandich, W.D. Reents, Jr.: J. Chem. Phys. **95**, 7360 (1991), and referencies cited therein
4. L.A. Bloomfield, R.R. Freeman, W.L. Brown: Phys. Rev. Lett. **54**, 2246 (1985)
5. Q.-L. Zhang, Y. Liu, R.F. Curl, F.K. Tittel, R.E. Smalley: J. Chem. Phys. **88**, 1670 (1988)
6. W. Begemann, K.H. Meiwes-Broer, H.O. Lutz: Phys. Rev. Lett. **56**, 2248 (1986)
7. M.F. Jarrold, E.C. Honea: J. Phys. Chem. **95**, 9181 (1991); M.F. Jarrold, J.E. Bower: J. Phys. Chem. **92**, 5702 (1988)
8. M.F. Jarrold, V.A. Constant: Phys. Rev. Lett. **67**, 2994 (1991); M.F. Jarrold, J.E. Bower: J. Chem. Phys. **96**, 9180 (1992)
9. J.M. Hunter, J.L. Fye, M.F. Jarrold, J.E. Bower: Phys. Rev. Lett. **73**, 2063 (1994)
10. K. Raghavachari, V. Logovinsky: Phys. Rev. Lett. **55**, 2853 (1985); K. Raghavachari, C.M. Rohlfing: J. Chem. Phys. **89**, 2219 (1988)
11. G. Pacchioni, J. Koutecky: J. Chem. Phys. **84**, 3301 (1986)
12. C.H. Patterson, R.P. Messmer: Phys. Rev. B **42**, 7530 (1990)
13. W. v. Niessen, V.G. Zakrzewski: J. Chem. Phys. **98**, 1271 (1993)
14. E. Kaxiras, K.A. Jackson: Z. Phys. D **26**, 349 (1993)
15. O. Cheshnovsky, S.H. Yang, C.L. Pettiette, M.J. Craycraft, Y. Liu, R.E. Smalley: Chem. Phys. Lett. **138**, 119 (1987)
16. T.N. Kitsopoulos, C.J. Chick, A. Weaver, D.M. Neumark: J. Chem. Phys. **93**, 6108 (1990)
17. G.R. Burton, C. Xu, C.C. Arnold, D.M. Neumark: J. Chem. Phys. **104**, 2757 (1996)
18. Y. Negishi, H. Kawamata, T. Hayase, M. Gomei, R. Kishi, F. Hayakawa, A. Nakajima, K. Kaya: Chem. Phys. Lett. **269**, 199 (1997)
19. C. Xu, T.R. Taylor, G.R. Burton, D.M. Neumark: J. Chem. Phys. **108**, 1395 (1998)
20. E.C. Honea, J.S. Kraus, J.E. Bower, M.F. Jarrold: Z. Phys. D **26**, 141 (1993)
21. M.L. Mandich, K.D. Rinnen: Z. Phys. D **26**, 147 (1993)
22. K. Fuke, K. Tsukamoto, F. Misaizu: Z. Phys. D **26**, S204 (1993)
23. K. Fuke, K. Tsukamoto, F. Misaizu, M. Sanekata: J. Chem. Phys. **99**, 7805 (1993)
24. T.P. Martin, H. Schaber: J. Chem. Phys. **83**, 855 (1985)
25. J.R. Heath, Y. Liu, S.C. O'Brien, Q.-L. Zhang, R.F. Curl, R.E. Smalley: J. Chem. Phys. **83**, 5520 (1985)
26. D.A. Dixon, J.L. Gole: Chem. Phys. Lett. **188**, 560 (1992)
27. D. Dai, K. Balasubramanian: J. Phys. Chem. **96**, 9236 (1992); J. Chem. Phys. **108**, 4379 (1998)
28. C. Jo, K. Lee: J. Korean Phys. Soc. **29**, S107 (1996)
29. J. Menéndez: Phys. Rev. B **38**, 6305 (1988)